Original Article

Asiaticoside attenuates neonatal hypoxic–ischemic brain damage through inhibiting TLR4/NF-κB/STAT3 pathway

Yu Zhou, Si Wang, Jing Zhao, Ping Fang

Department of Pediatrics, Affiliated Hospital of North Sichuan Medical College, Nanchong 637000, China

Contributions: (I) Conception and design: Y Zhou, J Zhao; (II) Administrative support: S Wang; (III) Provision of study materials or patients: Y Zhou, J Zhao, P Fang; (IV) Collection and assembly of data: All authors; (V) Data analysis and interpretation: Y Zhou, S Wang, P Fang; (VI) Manuscript writing: All authors; (VII) Final approval of manuscript: All authors.

Correspondence to: Jing Zhao. Department of Pediatrics, Affiliated Hospital of North Sichuan Medical College. No. 63, Cultural Road, Shunqing District, Nanchong 637000, China. Email: zhaojingjzj@163.com.

Background: Neonatal hypoxic ischemic encephalopathy (HIE) is currently a leading cause of neonatal death. Asiaticoside (AT), a bioactive constituent isolated from *Centella asiatica*, possesses numerous biological properties. For instance, previous studies showed that AT could protect ischemia hypoxia neurons by mediating BCL-2 protein. However, the roles and underlying mechanisms of AT in neonatal HIE have not been clarified.

Methods: Rice-Vannucci was applied to construct a hypoxic-ischemic brain damage (HIBD) model. Pathological damage of brain neuron tissue was determined by hematoxylin-eosin (HE) staining, while apoptosis was evaluated by terminal-deoxynucleoitidyl transferase nick end labeling (TUNEL) staining. Western blot and immunohistochemistry were applied to monitor related proteins levels. Enzyme-linked immunosorbent assay (ELISA) was conducted to measure the expression levels of inflammatory cytokines.

Results: The present study indicated that AT dose-dependently ameliorated histologic damage and inhibited apoptosis induced by hypoxic ischemia (HI) ($P<0.01$). AT also dose-dependently alleviated oxidative damage and reduced the levels of proinflammatory cytokines (ICAM-1, IL-18, and IL-1β) and TLR4 level. In terms of mechanism, decrease of TLR and IL-18 suppressed NF-κB phosphorylation and reduced the levels of TNFα, IL-6, and p-STAT3, leading to the inactivation of NF-κB/STAT3 pathway. Interestingly, with the addition of lipopolysaccharide (LPS), the increase of TLR4 activated NF-κB/STAT3 pathway again.

Conclusions: Collectively, the data provide insight into a novel mechanism by which AT may be an effective agent for HIE via the TLR4/NF-κB/STAT3 pathway.

Keywords: Asiaticoside (AT); neonatal hypoxic-ischemic brain damage (HIBD); TLR4; NF-κB; STAT3

Submitted Mar 19, 2020. Accepted for publication May 07, 2020.

doi: 10.21037/atm-20-3323

View this article at: http://dx.doi.org/10.21037/atm-20-3323

Introduction

Neonatal hypoxic-ischemic encephalopathy (HIE) is a clinical syndrome caused by long-term cerebral hypoxic ischemia in premature or full-term infants before birth or at birth (1). HIE can cause neurological sequelae such as cerebral palsy, cognitive impairment, stunting, and epilepsy, which can lead to death in severe cases (2,3). HIE is currently the leading cause of infant mortality. Its incidence ranges from 1–2‰ in full-term births (4). Currently, hypothermia is regarded as the only possible way for treating neonatal cerebrovascular injury in the perinatal period (5,6). However, only 50% of treatments are partially effective, with almost all the others having adverse outcomes (7). Therefore, it is still necessary to explore new treatment methods for neonatal HIE.

Asiaticoside (AT) is a bioactive constituent isolated from the medicinal plant, *Centella asiatica*. Accumulating

evidence suggests that AT has various biological effects, including neuroprotection (8), anti-ulceration (9), promotion of wound-healing (10-12), anti-inflammation, and antioxidation (13,14). Extensive research indicates that AT dramatically impacts various diseases such as osteolytic bone diseases (15), multiple sclerosis (16), Alzheimer's disease (13), oral lichen planus (8,17), and pulmonary hypertension (18). It has been previously documented that AT could protect ischemia hypoxia neurons by mediating BCL-2 protein *in vitro* (8). However, the specific roles and underlying molecular mechanisms in hypoxic-ischemic-induced neonatal encephalopathy are not well understood.

Toll-like receptors (TLRs), as part of the transmembrane receptor superfamily, are widely distributed in the central nervous system and play an important role in the induction and regulation of immune inflammatory response (19). For example, deficiency of TLR4 can reduce the expression of relevant inflammatory factors and thus alleviate the injury caused by inflammation. On the contrary, previous studies have shown that overexpression of TLR4 could promote neuronal cell death, indicating TLR4 participates in the regulation of brain injury in fetal and newborn rats (20,21). As a crucial regulatory factor, nuclear factor-kappa B (NF-κB) is involved in many physiological processes, such as immune response, apoptosis, tumor formation, and inflammatory response. Activation of TLR4 can induce the phosphorylation of NF-κB and migration into the nucleus, thereby attenuating neuronal autophagy and inflammatory injury in experimental traumatic brain injury (22). Signal transducer and activator of transcription 3 (STAT3) also plays key roles in the occurrence of brain inflammation (23). Researches showed that AT possessed inhibitory effect on TLR4/NF-κB signaling pathway. Song *et al.* found that AT can attenuate Aβ1-42 induced cell growth inhibition and apoptosis in human brain microvascular endothelial cells via inhibiting the TLR4/NF-κB signaling pathway (24). Xing *et al.* reported that AT could protect cochlear hair cells from high glucose-induced oxidative stress via suppressing AGEs/RAGE/NF-κB pathway (25). Nevertheless, as an important signal pathway, whether TLR4/NF-κB/STAT3 pathway participates in neonatal HIE is still not clear.

To date, the specific roles and potential molecular mechanisms of AT in neonatal HIE have still not been determined. In the present study, we first explored the role of AT in neonatal HI-induced brain damage, and then subsequently examined the underlying mechanisms *in vivo*. Overall, this study is the first to provide direct evidence for the potential of AT as a promising therapeutic agent in HIE. We present the following article in accordance with the ARRIVE reporting checklist (available at http://dx.doi.org/10.21037/atm-20-3323).

Methods

Hypoxic-ischemic brain damage (HIBD) animal models

All animal experiments were carried out in accordance with the National Institutes of Health (NIH) Guide for the Care and Use of Laboratory Animals and were approved by the Affiliated Hospital of North Sichuan Medical College. A total of 70 Sprague-Dawley rats [male, on postnatal day (P) 7 (P7), weight range 13–17 g] were obtained from the Animal Center of the Affiliated Hospital of North Sichuan Medical College. In this study, we used Rice-Vannucci to construct a HIBD model. The rats were anesthetized with an intraperitoneal injection of ketamine (25 mg/kg) and xylazine (5 mg/kg) (26). The left common carotid artery was exposed, isolated from the vagus nerve, and double-ligated with 4-0 surgical silk. The procedure was completed within 10 min. After being sutured, the rats recovered for 1 hour, and were placed in a hypoxia chamber with 8% oxygen balanced with nitrogen at 37 ℃ for 2 hours. After successful modeling, the mice were randomly divided into the 7 following groups with 10 mice in each group: the control group, healthy rats; the HIBD group, HIBD models; the HIBD + AT (10 mg) group, HIBD models given 10 mg/kg AT; the HIBD + AT (20 mg) group, HIBD models given mg/kg AT; the HIBD + AT (40 mg) group, HIBD models given mg/kg AT; the HIBD + lipopolysaccharides (LPS) group, HIBD models injected with 0.4 mg/kg LPS; the HIBD + LPS + AT (40 mg), HIBD models injected with 0.4 mg/kg LPS and given 40 mg/kg AT. After injection for 25 days, the rats were anesthetized, rats were sacrificed by decapitation immediately and brains were rapidly removed. The cortical tissues of the left hemispheres were dissected on ice, frozen immediately on dry ice, and then stored at –80 ℃ for subsequent experiments.

Hematoxylin and eosin (HE) staining

Brain neuron tissue was fixed in 4% formaldehyde for 72 hours. After being decalcified in 20% ethylenediamine tetra acetic acid, the sample was dehydrated in gradient concentrations of ethanol and embedded in paraffin. Then, the tissues were cut into 5-μm slices and dyed with HE staining. The HE-stained sections were observed with a

light microscope for morphologic changes (BX51; Olympus Corp., Tokyo, Japan). All experiments were repeated 3 times.

Terminal-deoxynucleoitidyl transferase nick end labeling (TUNEL) assay

Neuronal apoptosis in hippocampal CA1 region was examined with the TUNEL assay (Beyotime, Jiangsu, China) in accordance with the manufacturer's instruction. Coronal sections were taken from the middle part of the optic chiasm and papillary body. The apoptotic neurons in hippocampal CA1 area were observed in 5 random visual fields with microscopy. The apoptotic cells were counted by Image-Pro Plus 5.1 image analysis software (27). All experiments were repeated 3 times.

Western blot assays

Brain neuron tissue was ground in liquid nitrogen and lysed in the lysis buffer. (Beyotime, Shanghai, China) The concentrations of proteins were determined using a Pierce BCA Protein Assay Kit. (Thermo Fisher Scientific, Inc.) Samples were separated via 10% SDS-PAGE and transferred to polyvinylidene difluoride membranes (EMD Millipore, Billerica, MA, USA). After blocking with 5% bovine serum albumin (BSA) for 1 hour at room temperature, the samples were probed with primary antibodies against GAPDH (#5174, 1:1,000, Cell Signaling Technology, MA, USA), caspase-3 (#9665, 1:1,000, CST, MA, USA), caspase-9 (#9508, 1:1,000, CST, MA, USA), NF-κB p65 (#8242, 1:1,000, CST, MA, USA), p-p65 (#3033, 1:1000, CST, MA, USA), STAT3 (#9139, 1:1,000, CST, MA, USA) p-STAT3 (#9145, 1:2,000, CST, MA, USA), TNF-α (#3707, 1:1,000, CST, MA, USA), and TLR4 (#14358, 1:1,000, CST, MA, USA), ICAM-1 (#4915, 1:1,000, CST, MA, USA), at 4 ℃ overnight. The next day, membranes were incubated with anti-rabbit IgG (H + L) secondary antibody (#14708, 1:1,000, CST, MA, USA) for 1.5 hours at room temperature. Proteins were visualized using enhanced chemiluminescence reagents (Pierce, USA). Analysis was performed using ImageJ software (version 1.48, National Institutes of Health, Bethesda, MD, USA). All experiments were repeated 3 times.

Lactate dehydrogenase (LDH), superoxide dismutase (SOD), and malondialdehyde (MDA) measurement

Serum was collected from each group and stored at –80 ℃ for analysis. Serum LDH, SOD, and MDA were determined by the following methods. The release rate of (LDH) was determined by spectrophotometer. Activities of (SOD) activity were measured by xanthine oxidase, and content of (MDA) was determined by thiobarbital colorimetry. All the operation steps were conducted according to the manufacturer's instructions (Vazyme, China). All experiments were repeated 3 times.

Immunohistochemical (IHC) analysis

IHC analysis was conducted as previously described (28). Briefly, 5 μm-thick paraffin sections were deparaffinized in xylene and rehydrated in ethanol at several different gradients. The slices were heated in citrate for 10 minutes and then cooled for 30 minutes. After that, the sections were incubated in 3% H_2O_2 for 10 minutes to inactivate endogenous peroxidase. After dropping 100–400 μL of preferred sealing liquid on each slice and sealing for 1 hour at room temperature, the slices were incubated with primary antibody of intercellular adhesion molecule-1 (ICAM-1) (anti-ICAM-1, #4915, 1:25, CST, USA) at 4 ℃ overnight. Corresponding secondary antibody was then added for 1 hour at room temperature. The images were observed under a light microscope. All experiments were repeated 3 times.

Enzyme-linked immunosorbent assay (ELISA)

Serum were collected from each group and stored at –80 ℃ for analysis. Cytokines including interleukin-6 (IL-6), interleukin-18 (IL-18), and interleukin-1β (IL-1β) were measured with ELISA kits according to the manufacturer's instructions (Bio-Swamp, Shanghai, China). A microplate reader (BioTek Epoch, Winooski, VT, USA) was used to detect the optical density (OD) values at 450 nm. Quantitative analysis of IL-6, IL-18, and IL-1β were measured according to the standard curve. All experiments were repeated 3 times.

Statistical analysis

Data are presented as the mean ± standard deviation of experiments repeated at least 3 times. Statistical comparisons between different groups were conducted using one-way analysis of variance followed by Bonferroni's post hoc test using SPSS 13.0 (SPSS, Inc., Chicago, IL, USA). A P value <0.05 was considered to indicate a

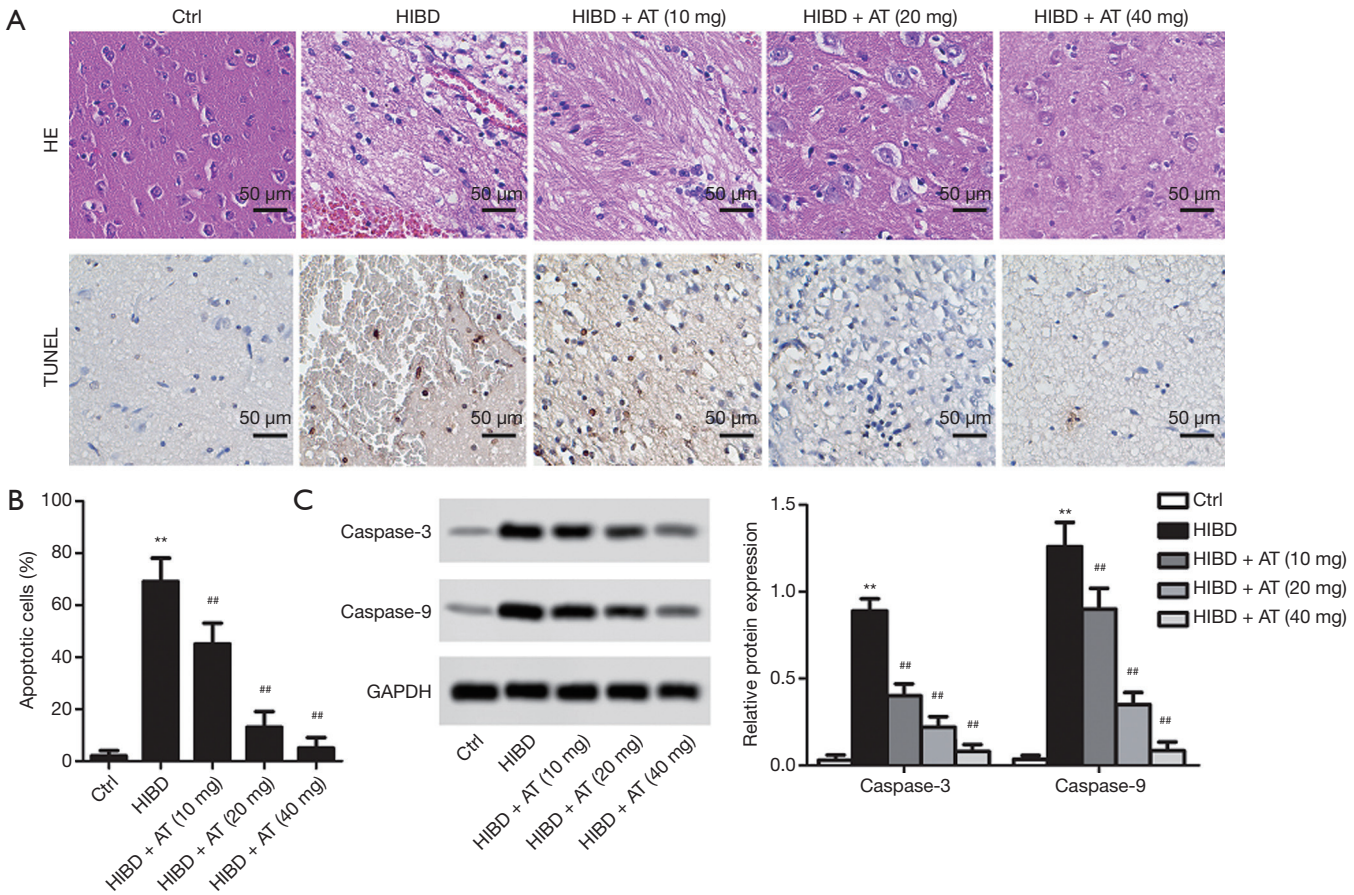

Figure 1 AT mitigated HI-induced brain neurons damage and apoptosis. Mice were randomly divided into the 7 following groups with 10 mice in each group: the control group, healthy rats; the HIBD group, hypoxic-ischemic brain damage models; the HIBD + AT (10 mg) group, the HIBD models given 10 mg/kg AT; the HIBD + AT (20 mg) group, HIBD models given mg/kg AT; the HIBD + AT (40 mg) group, HIBD models given mg/kg AT. (A) HE staining showed the histological changes in each group. (B) TUNEL staining showed the apoptosis in each group. The bar graph represents the percentage of apoptotic cells. (C) The expression of apoptosis marker proteins caspase-3 and caspase-9 in each group were measured by Western blot. The bar graph represents the relative protein expression level. Each experiment included 4 repetitions per condition (**, P<0.01 *vs.* control group; ##, P<0.01 *vs.* HIBD group). AT, asiaticoside; HIBD, hypoxic-ischemic brain damage; TUNEL, terminal-deoxynucleoitidyl transferase nick end labeling.

statistically significant difference.

Results

AT mitigated HI-induced brain neuron damage and apoptosis

In the HE staining, the cell contour of brain neuron tissue in the control group was clear and normal with the nucleus in the center and the Nissl bodies distributed uniformly around the nucleus. In the HI-induced HIBD group, the brain neuron tissue was atrophic and pale, with a thin cortex and the formation of a few voids. Furthermore, neurons were lost, and glial scars were formed in the cortex of the hippocampus and thalamus. However, with the treatment of AT, the pathological changes were obviously ameliorated in a dose-dependent manner (*Figure 1A*). Similarly, TUNEL staining exhibited that more brown nuclei were observed in hippocampal CA1 area in the HI-induced HIBD group compared with the control group. However, with the addition of AT, brown nuclei were dose-dependently decreased (*Figure 1B*, **P<0.01, ##P<0.01). Furthermore, western blot also showed that apoptosis marker protein level (Caspase-3 and Caspase-9) were also dose-dependently

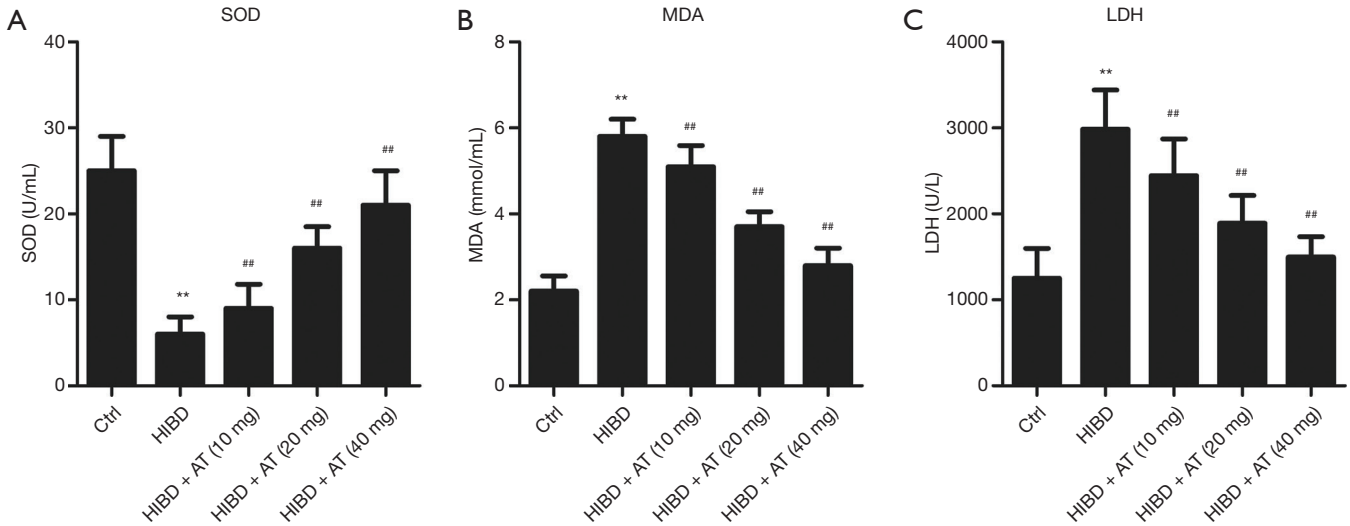

Figure 2 AT alleviated HI-induced oxidative damage. Mice were randomly divided into the 7 following groups with 10 mice in each group: the control group, healthy rats; the HIBD group, hypoxic-ischemic brain damage models; the HIBD + AT (10 mg) group, the HIBD models given 10 mg/kg AT; the HIBD + AT (20 mg) group, HIBD models given mg/kg AT; the HIBD + AT (40 mg) group, HIBD models given mg/kg AT. (A) Activity of SOD in each group. (B) The accumulation of MDA in each group. (C) Release rate of LDH in each group (**, P<0.01 *vs.* control; ##, P<0.01 *vs.* HIBD group). AT, asiaticoside; HIBD, hypoxic-ischemic brain damage; SOD, superoxide dismutase; MDA, malondialdehyde; LDH, lactate dehydrogenase.

inhibited with the treatment of AT (*Figure 1C*, **P<0.01, ##P<0.01), which was consistent with TUNEL staining.

AT alleviated HI-induced oxidative damage

Oxidative damage is the major mechanism for HI-induced brain neuron damage. The release rate of LDH was determined by spectrophotometer. As shown in *Figure 2*, activities of SOD were significantly reduced in the HI-induced HIBD group compared with the control group, while MDA content and LDH release rate were significantly increased, indicating the damaging effects of hypoxia and ischemia (*Figure 2A,B,C*, **P<0.01, ##P<0.01). However, AT treatment enhanced activities of SOD, and decreased HI-induced MDA accumulation and the release of LDH in a dose-dependent manner compared with the HIBD group (**P<0.01, ##P<0.01). Overall, these results demonstrate that AT had an inhibitory effect on HI-induced oxidative damage.

AT reduced HI-induced proinflammatory cytokines levels

Intercellular adhesion molecule-1 (ICAM-1) is the main pro-inflammatory factor after brain injury, and is involved in the inflammatory response in the reperfusion area. Immunohistochemistry assay revealed that the expression of ICAM-1 was elevated in the HI-induced HIBD group compared with the control. However, with the addition of AT, expression of ICAM-1 was dose-dependently decreased (*Figure 3A* and *B*; **P<0.01; ##P<0.01). Parallelly, we also examined the levels of ICAM-1 using Western blot assay, and the results were consistent with IHC (*Figure 3C*). Additionally, serum proinflammatory cytokine levels of IL-6, IL-18, and IL-1β were also identified using ELISA assays. The results demonstrated that serum pro-inflammatory cytokines levels (IL-6, IL-18, and IL-β) were significantly increased in HI-induced HIBD group compared with the control. However, adding AT counteracted the increase of IL-6, IL-18, and IL-1β (*Figure 3D*; **P<0.01; ##P<0.01). All these results indicate that AT reduced HI-induced proinflammatory cytokine levels and might effectively protect against HI-induced brain damage.

TLR4/NF-κB/STAT3 pathway was implicated in the activity of AT in HI-induced brain damage

In a further investigation of the related molecular mechanisms, activation of TLR4/NF-κB/STAT3 pathway

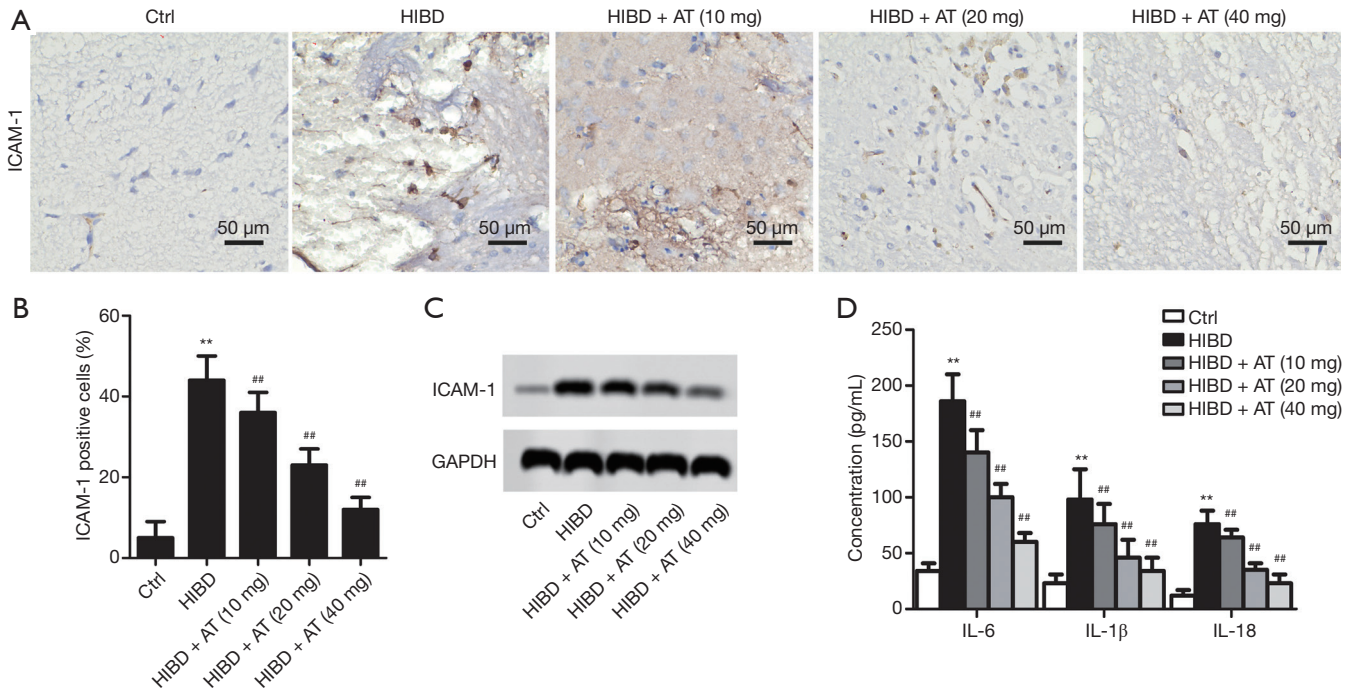

Figure 3 AT reduced HI-induced proinflammatory cytokines levels. Mice were randomly divided into the 7 following groups with 10 mice in each group: the control group, healthy rats; the HIBD group, hypoxic-ischemic brain damage models; the HIBD + AT (10 mg) group, the HIBD models given 10 mg/kg AT; the HIBD + AT (20 mg) group, HIBD models given mg/kg AT; the HIBD + AT (40 mg) group, HIBD models given mg/kg AT. (A) ICAM-1 was examined by using immunohistochemical analysis in each group. (B) The bar graph represents the percentage of ICAM-1 positive cells in each group. (C) The expression of pro-inflammatory factor ICAM-1 in each group were measured by Western blot. (D) The levels of IL-6, IL-18, and IL-1β were detected by ELISA assay in each group (**, P<0.01 *vs.* control; ##, P<0.01 *vs.* HIBD group). AT, asiaticoside; HIBD, hypoxic-ischemic brain damage; ICAM-1, intercellular adhesion molecule-1; ELISA, enzyme-linked immunosorbent assay.

was measured by western blot. As shown in *Figure 4A* and *B*, compared with the control, TLR4 level was markedly increased in the HIBD group, and the enhanced TLR4 further promoted the phosphorylation of NF-κB and STAT3 as well as TNFα level. However, treatment with AT for 40 mg/kg greatly decreased TLR4 level, the decrease of TLR4 further inhibited phosphorylation of NF-κB and STAT3, while reducing TNFα level (**P<0.01; ##P<0.01). Taken together, these results indicate that AT inhibited HI-induced brain damage via inactivating TLR4/NF-κB/STAT3 pathway.

LPS decreased the inhibition of AT to HI-induced brain damage via activating TLR4/NF-κB/STAT3 signaling pathway

To further confirm the involvement of TLR4/NF-κB/STAT3 pathway, the TLR4-specific activator, LPS, was injected into the caudal vein of the rats. As shown in *Figure 5A*, with the addition of LPS, TLR4 level was elevated, and the elevated TLR4 further promoted phosphorylation of NF-κB and STAT3, in addition to increasing TNF-α when compared with the HIBD + AT (40 mg) group. This indicated that LPS weakened the suppressing effect of AT on the activation of TLR4/NF-κB/STAT3 pathway. However, the combined treatment of LPS and AT counteracted the inhibition of AT on the activation of TLR4/NF-κB/STAT3 pathway to some extent (**P<0.01; ##P<0.01; &&P<0.01) Furthermore, HE staining showed that with the treatment of LPS, brain neuron tissue deteriorated, and astrocytes proliferated with neurons being lost in large numbers (*Figure 5B*). Additionally, adding LPS enhanced the expression of IL-6 and decreased the activities of SOD (*Figure 5C* and *D*, **P<0.01; ##P<0.01; &&P<0.01).

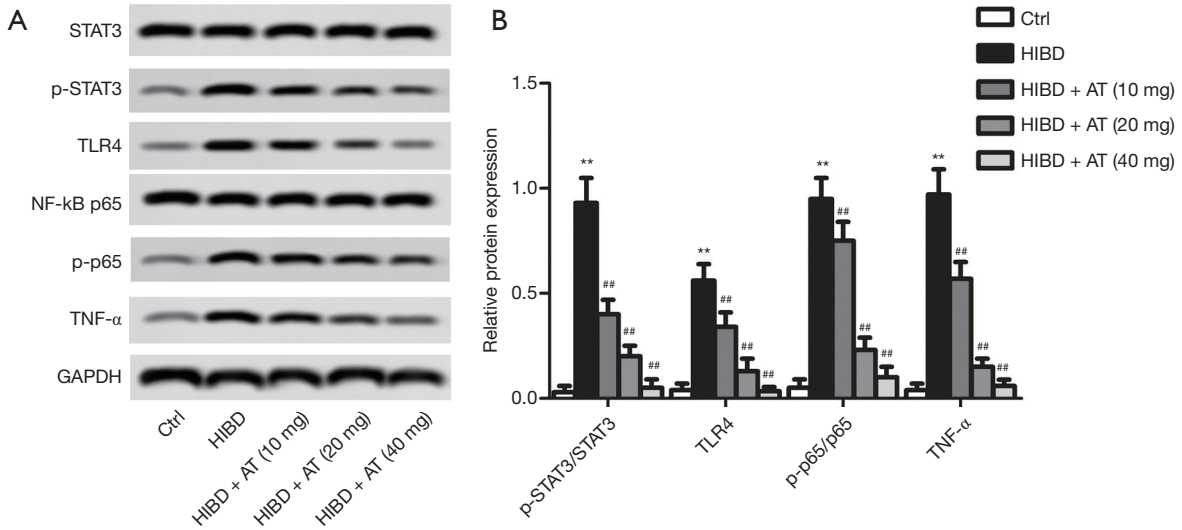

Figure 4 TLR4/NF-κB/STAT3 pathway was implicated in the activity of AT in HI-induced brain damage. Mice were randomly divided into the 7 following groups with 10 mice in each group: the control group, healthy rats; the HIBD group, hypoxic-ischemic brain damage models; the HIBD + AT (10 mg) group, the HIBD models given 10 mg/kg AT; the HIBD + AT (20 mg) group, HIBD models given mg/kg AT; the HIBD + AT (40 mg) group, HIBD models given mg/kg AT. (A) For each group, the LPS-induced TLR4 and phosphorylation of NF-κB and STAT3, along with the TNF-α, was measured by Western blot. B. The bar graph represents the relative protein expression of p-STAT3/STAT3, TLR4, p-p65/p65, and TNF-α in each group. GAPDH was used as an internal control (**, P<0.01 *vs.* control; ##, P<0.01 *vs.* HIBD group). AT, asiaticoside; HIBD, hypoxic-ischemic brain damage.

Collectively, these results confirm that LPS decreased the inhibition of AT to HI-induced brain damage via activating TLR4/NF-κB/STAT3 signaling pathway.

Discussion

Hypoxia stimulates the release of glutamate, which not only causes epilepsy, but also increases the inflow of calcium ions. Change in calcium concentration activates the mitochondrial apoptotic pathway and stimulates the production of reactive oxygen species, thus causing hypoxic-ischemic-induced brain damage (29-32). HIBD often leads to permanent brain damage in human neonates, resulting in nervous system disability or even infantile mortality (33). Currently, hypothermia treatment is the only available treatment to improve the outcome of neonatal HIBD, However, hypothermia (HT) for neonatal HIBD is advised to start within the first 6 hours after birth. Besides hypothermia, our research found a bioactive compound to also be effective in the treatment of HIBD (34-36).

Chinese medical herbs are derived from a wide range of sources and natural substances, and afflict users with few side effects. AT, a bioactive ingredient extracted from *Centella asiatica*, has been regarded as an important agent in various diseases. In current studies, AT was reported to have a significant neuroprotective and anti-inflammatory effects (37-39). Previous studies reported that treatment with AT markedly reduced the level of the pro-inflammatory cytokines (IL-6, TNF-α, and IL-1β), repaired the damaged subcellular structure, and decreased caspase-3 expression (13,17). Moreover, in Luo *et al.*'s research, treating with AT observably decreased the level of MDA, and increased the level of SOD, glutathione (GSH), and glutathione-peroxidase (GSH-PX) (14). Another study revealed that AT was also involved in apoptosis (17,40). As reported in Song *et al.*'s research, pretreatment of AT (25, 50, and 100 mM) for 12 hours significantly attenuated apoptosis, and restored declining mitochondrial membrane potential in human brain microvascular endothelial cells (hBMECs) (17). Consistent with these results, our studies demonstrated that AT inhibited cell apoptosis and reduced the expression of pro-inflammatory cytokines and oxidative damage *in vivo*. Additionally, AT also restored the histological injuries in neonatal brain neurons. Taken together, our results support the notion that AT may be an effective agent for HIE clinically.

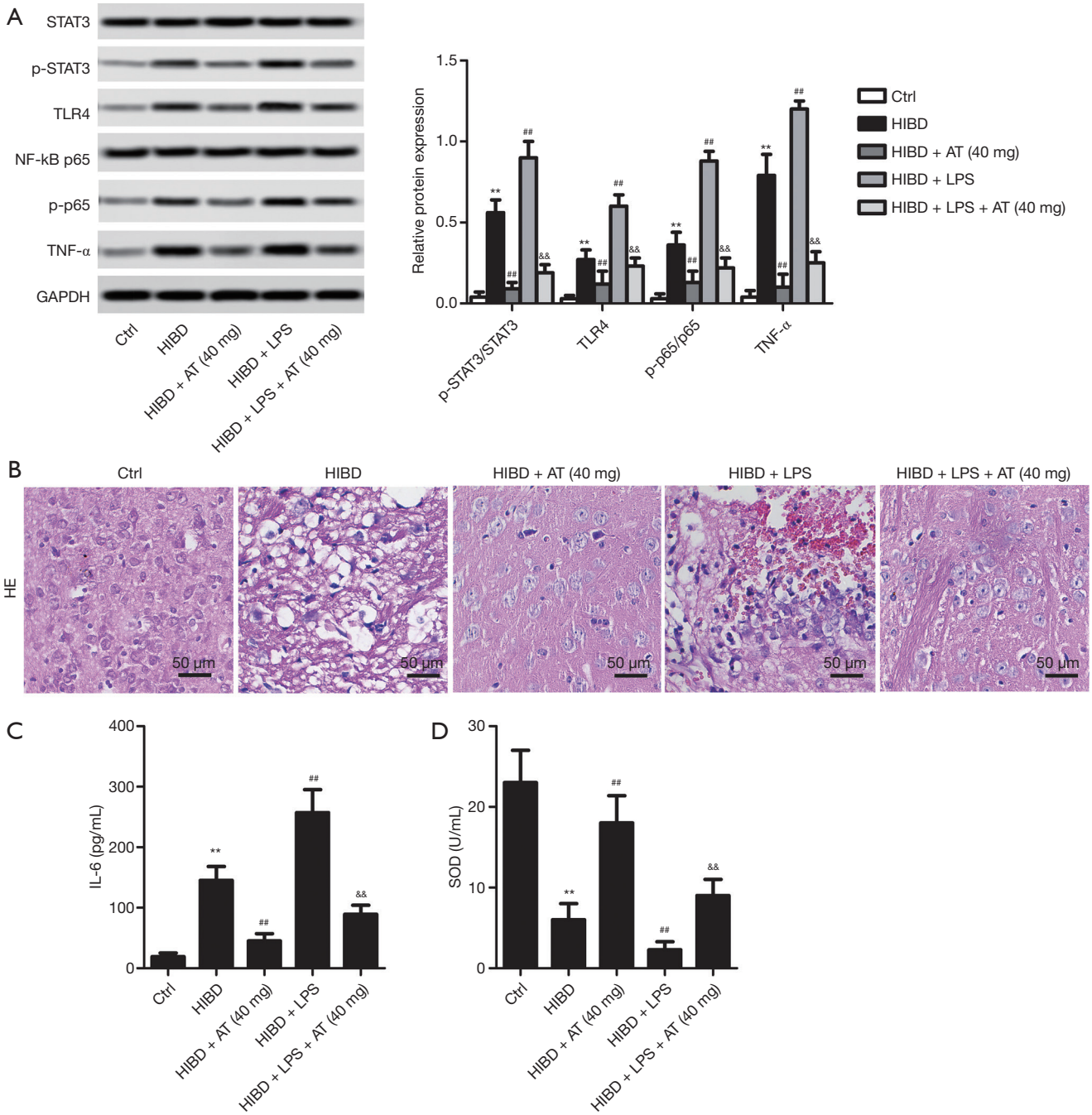

Figure 5 LPS decreased the inhibition of AT to HI-induced brain damage via activating TLR4/NF-κB/STAT3 signaling pathway. Mice were randomly divided into the 7 following groups with 10 mice in each group: the control group, healthy rats; the HIBD group, hypoxic-ischemic brain damage models; the HIBD + AT (10 mg) group, the HIBD models given 10 mg/kg AT; the HIBD + AT (20 mg) group, HIBD models given mg/kg AT; the HIBD + AT (40 mg) group, HIBD models given mg/kg AT. (A) Western blot assays were used to monitor the levels of TLR4, p-65, and p-STAT3 along with TNF-α. The bar graph represents the relative protein expression of p-STAT3/STAT3, TLR4, p-p65/p65, and TNF-α in all groups. GAPDH was used as an internal control. (B) HE staining clarified the role of LPS in HI-induced brain neuron tissue. (C) IL-6 level of each group was measured. (D) The SOD activity was assessed in each group (**, P<0.01 *vs.* control; ##, P<0.01 *vs.* HIBD group; &&, P<0.01 *vs.* HIBD + LPS group). LPS, liposaccharide; AT, asiaticoside; HIBD, hypoxic-ischemic brain damage; SOD, superoxide dismutase.

Numerous studies have demonstrated that TLR4/NF-κB/STAT3 pathway plays an important role in various cell processes, including cell proliferation and apoptosis (41-43). As a common signal pathway, TLR4/NF-κB was found to be regulated by numerous bioactive compounds (41,44). In Liao *et al.*'s research, LPS-induced anti-inflammatory factor level was restrained by chelidonine via inhibiting TLR4/NF-κB signaling pathway in RAW264.7 macrophages (45). Furthermore, in human endothelial cells, kaempferol alleviated ox-LDL-induced apoptosis through the inhibition of TLR4/NF-κB pathway (46). In addition, astrocytic GAP43 induced by the TLR4/NF-κB/STAT3 pathway attenuated astrogliosis-mediated microglial activation and neurotoxicity and provided beneficial effects for neuronal plasticity. Another study found that treating with resveratrol significantly reduced brain edema, motor deficit, neuronal loss, and improved spatial cognitive function by suppressing the TLR4/NF-κB signaling pathway. Likewise, in our studies, we found that AT notably decreased the protein levels of TLR4 and IL-18, while the decreased levels of TLR4 and IL-18 further inhibited the phosphorylation of NF-κB. The inhibition of p-NF-κB in turn suppressed the level of TNF-α and IL-6, thus leading to the inhibition of STAT3 phosphorylation. On the whole, the results strongly suggest that the TLR4/NF-κB/STAT3 pathway was obstructed by AT. Furthermore, with the addition of LPS, the TLR4/NF-κB/STAT3 pathway was activated again.

Conclusions

In conclusion, our results revealed a novel mechanism of AT in HIBD. In the present study, we proved that AT (10, 20, and 40 mg/kg) significantly inhibited HIBD-induced apoptosis, reduced the levels of pro-inflammatory cytokines, and further repaired brain neuron injury and oxidative damage in a dose-dependent manner via the TLR4/NF-κB/STAT3 pathway. Our study provides insights into a novel mechanism by which AT may be an effective agent for HIE clinically.

Acknowledgments

Funding: This study was partially supported by the National Natural Science Foundation of China (No. 81300528).

Footnote

Reporting Checklist: The authors have completed the ARRIVE reporting checklist. Available at http://dx.doi.org/10.21037/atm-20-3323

Data Sharing Statement: Available at http://dx.doi.org/10.21037/atm-20-3323

Conflicts of Interest: All authors have completed the ICMJE uniform disclosure form (available at http://dx.doi.org/10.21037/atm-20-3323). The authors have no conflicts of interest to declare.

Ethical Statement: The authors are accountable for all aspects of the work in ensuring that questions related to the accuracy or integrity of any part of the work are appropriately investigated and resolved. The study was approved by the Affiliated Hospital of North Sichuan Medical College.

References

1. Dani C, Poggi C, Fancelli C, et al. Changes in bilirubin in infants with hypoxic-ischemic encephalopathy. Eur J Pediatr 2018;177:1795-801.
2. Badawi N, Felix JF, Kurinczuk JJ, et al. Cerebral palsy following term newborn encephalopathy: a population-based study. Develop Med Child Neurol 2005;47:293-8.
3. Cowan F, Rutherford M, Groenendaal F, et al. Origin and timing of brain lesions in term infants with neonatal encephalopathy. Lancet 2003;361:736-42.
4. Volpe JJ. Neonatal encephalopathy: An inadequate term for hypoxic-ischemic encephalopathy. Ann Neurol 2012;72:156-66.
5. Azzopardi DV, Strohm B, Edwards AD, et al. Moderate hypothermia to treat perinatal asphyxial encephalopathy. N Engl J Med 2009;361:1349-58.
6. Jacobs SE, Hunt R, Tarnow-Mordi WO, et al. Cooling for newborns with hypoxic ischaemic encephalopathy. John Wiley & Sons, Ltd., 2007.
7. Edwards AD, Brocklehurst P, Gunn AJ, et al. Neurological

outcomes at 18 months of age after moderate hypothermia for perinatal hypoxic ischaemic encephalopathy: synthesis and meta-analysis of trial data. BMJ 2010;340:c363.
8. Sun T, Liu B, Li P. Nerve Protective Effect of Asiaticoside against Ischemia-Hypoxia in Cultured Rat Cortex Neurons. Med Sci Monit 2015;21:3036-41.
9. Guo JS, Cheng CL, Koo MW. Inhibitory effects of Centella asiatica water extract and asiaticoside on inducible nitric oxide synthase during gastric ulcer healing in rats. Planta Medica 2004;70:1150-4.
10. Lee JH, Kim HL, Mi HL, et al. Asiaticoside enhances normal human skin cell migration, attachment and growth in vitro wound healing model. Phytomedicine 2012;19:1223-7.
11. Hou Q, Li M, Lu YH, et al. Burn wound healing properties of asiaticoside and madecassoside. Exp Ther Med 2016;12:1269-74.
12. Verma N, Kumari U, Mittal S, et al. Effect of asiaticoside on the healing of skin wounds in the carp Cirrhinus mrigala: An immunohistochemical investigation. Tissue Cell 2017;49:734-45.
13. Zhang Z, Li X, Li D, et al. Asiaticoside ameliorates β-amyloid-induced learning and memory deficits in rats by inhibiting mitochondrial apoptosis and reducing inflammatory factors. Exp Ther Med 2017;13:413-20.
14. Luo Y, Fu C, Wang Z, et al. Asiaticoside attenuates the effects of spinal cord injury through antioxidant and anti-inflammatory effects, and inhibition of the p38-MAPK mechanism. Mol Med Rep 2015;12:8294.
15. He L, Hong G, Zhou L, et al. Asiaticoside, a component of Centella asiatica attenuates RANKL-induced osteoclastogenesis via NFATc1 and NF-kappaB signaling pathways. J Cell Physiol 2019;234:4267-76.
16. Madhu K, T P. Asiaticoside counteracts the in vitro activation of microglia and astrocytes: Innuendo for multiple sclerosis. Biomed Pharmacother 2018;107:303-5.
17. Song D, Jiang X, Liu Y, et al. Asiaticoside Attenuates Cell Growth Inhibition and Apoptosis Induced by Aβ1-42via Inhibiting the TLR4/NF-κB Signaling Pathway in Human Brain Microvascular Endothelial Cells. Frontiers Pharmacol 2018;9:28.
18. Wang X, Cai X, Wang W, et al. Effect of asiaticoside on endothelial cells in hypoxiainduced pulmonary hypertension. Mol Med Rep 2018;17:2893-900.
19. Vartanian K, Stenzelpoore M. Toll-like receptor tolerance as a mechanism for neuroprotection. Transl Stroke Res 2010;1:252-60.
20. Barboza R, Lima FA, Reis AS, et al. TLR4-Mediated Placental Pathology and Pregnancy Outcome in Experimental Malaria. Sci Rep 2017;7:8623.
21. Church JS, Kigerl KA, Lerch JK, et al. TLR4 Deficiency Impairs Oligodendrocyte Formation in the Injured Spinal Cord. J Neurosci 2016;36:6352-64.
22. Yan F, Ying C, Gao JL, et al. Resveratrol attenuates neuronal autophagy and inflammatory injury by inhibiting the TLR4/NF-κB signaling pathway in experimental traumatic brain injury. Inter J Mol Med 2016;37:921-30.
23. Sofroniew MV. Molecular dissection of reactive astrogliosis and glial scar formation. Trends Neurosci 2009;32:638-47.
24. Song D, Jiang X, Liu Y, et al. Asiaticoside Attenuates Cell Growth Inhibition and Apoptosis Induced by Aβ1-42 via Inhibiting the TLR4/NF-κB Signaling Pathway in Human Brain Microvascular Endothelial Cells. Front Pharmacol 2018;9:28.
25. Xing Y, Ji Q, Li X, et al. Asiaticoside protects cochlear hair cells from high glucose-induced oxidative stress via suppressing AGEs/RAGE/NF-κB pathway. Biomed Pharmacother 2017;86:531-6.
26. Sakai T, Sasaki M, Kataoka-Sasaki Y, et al. Functional recovery after the systemic administration of mesenchymal stem cells in a rat model of neonatal hypoxia-ischemia. J Neurosurg Pediatr 2018;22:513-22.
27. Tatlipinar S, Soylemezoglu F, Kiratli H, et al. Quantitative analysis of apoptosis in retinoblastoma. China Social Sciences Press, 2002.
28. Liao T, Qu N, Shi RL, et al. BRAF-activated LncRNA functions as a tumor suppressor in papillary thyroid cancer. Oncotarget 2016;8:238-47.
29. Vannucci SJ, Hagberg H. Hypoxia-ischemia in the immature brain. J Exp Biol 2004;207:3149-54.
30. Abe S, Fujioka K. Mesenchymal stem cell therapy for neonatal intraventricular hemorrhage: a long way to go? Ann Transl Med 2019;7:79.
31. Semple BD, Blomgren K, Gimlin K, et al. Brain development in rodents and humans: Identifying benchmarks of maturation and vulnerability to injury across species. Prog Neurobiol 2013;106-107:1-16.
32. Blomgren K, Hagberg H. Free radicals, mitochondria, and hypoxia-ischemia in the developing brain. Free Radic Biol Med 2006;40:388-97.
33. Yasuhara T, Matsukawa N, Yu G, et al. Behavioral and histological characterization of intrahippocampal grafts of human bone marrow-derived multipotent progenitor cells in neonatal rats with hypoxic-ischemic injury. Cell Transplant 2006;15:231-8.
34. Yenari M, Kitagawa K, Lyden P, et al. Metabolic

downregulation: a key to successful neuroprotection? Stroke 2008;39:2910-7.
35. Shankaran S, Laptook A, Wright LL, et al. Wholebody hypothermia for neonatal encephalopathy: animal observations as a basis for a randomized, controlled pilot study in term infants. Pediatrics 2002;110:377.
36. Sabir H, Scullbrown E, Liu X, et al. Immediate hypothermia is not neuroprotective after severe hypoxia-ischemia and is deleterious when delayed by 12 hours in neonatal rats. Stroke 2012;43:3364-70.
37. Qi FY, Yang L, Tian Z, et al. Neuroprotective effects of Asiaticoside. Neural Regen Res 2014;9:1275-82.
38. Gopi M, Arambakkam Janardhanam V. Asiaticoside: Attenuation of rotenone induced oxidative burden in a rat model of hemiparkinsonism by maintaining the phosphoinositide-mediated synaptic integrity. Pharmacol Biochem Behav 2017;155:1-15.
39. Jing L, Haitao W, Qiong W, et al. Anti inflammatory effect of asiaticoside on human umbilical vein endothelial cells induced by ox-LDL. Cytotechnology 2018;70:855-64.
40. Song D, Jiang X, Liu Y, et al. Asiaticoside Attenuates Cell Growth Inhibition and Apoptosis Induced by Aβ via Inhibiting the TLR4/NF-κB Signaling Pathway in Human Brain Microvascular Endothelial Cells. Front Pharmacol 2018;9:28.
41. Capiralla H, Vingtdeux V, Zhao H, et al. Resveratrol mitigates lipopolysaccharide- and Abeta-mediated microglial inflammation by inhibiting the TLR4/NF-kappaB/STAT signaling cascade. J Neurochem 2012;120:461-72.
42. Jiang Y, Zhou J, Luo P, et al. Prosaposin promotes the proliferation and tumorigenesis of glioma through toll-like receptor 4 (TLR4)-mediated NF-kappaB signaling pathway. EBioMedicine 2018;37:78-90.
43. Wang CH, Wang PJ, Hsieh YC, et al. Resistin facilitates breast cancer progression via TLR4-mediated induction of mesenchymal phenotypes and stemness properties. Oncogene 2018;37:589-600.
44. Shalini V, Jayalekshmi A, Helen A. Mechanism of anti-inflammatory effect of tricin, a flavonoid isolated from Njavara rice bran in LPS induced hPBMCs and carrageenan induced rats. Mol Immunol 2015;66:229-39.
45. Liao W, He X, Yi Z, et al. Chelidonine suppresses LPS-Induced production of inflammatory mediators through the inhibitory of the TLR4/NF-kappaB signaling pathway in RAW264.7 macrophages. Biomed Pharmacother 2018;107:1151-9.
46. Zhong X, Zhang L, Li Y, et al. Kaempferol alleviates ox-LDL-induced apoptosis by up-regulation of miR-26a-5p via inhibiting TLR4/NF-kappaB pathway in human endothelial cells. Biomed Pharmacother 2018;108:1783-9.

Cite this article as: Zhou Y, Wang S, Zhao J, Fang P. Asiaticoside attenuates neonatal hypoxic–ischemic brain damage through inhibiting TLR4/NF-κB/STAT3 pathway. Ann Transl Med 2020;8(10):641. doi: 10.21037/atm-20-3323

